Heterogeneous Inhibition of Homogeneous Reactions: Karstedt Catalyzed Hydrosilylation

Francesco Faglioni,† Mario Blanco, William A. Goddard, III,* and Dennis Saunders
Materials and Process Simulation Center, Beckman Institute (139-74), Caltech, Pasadena, California 91125, and Avery Research Center, Pasadena, California 91107

Received: July 26, 2001; In Final Form: November 26, 2001

The Karstedt-catalyzed hydrosilylation reaction used in curing of silicone release coatings was investigated using first-principle quantum mechanical techniques (density functional theory) as well as semiempirical methods to estimate solubility parameters. The results we obtain for the catalytic cycle indicate, in agreement with experimental results, that hydrosilylation occurs easily at room temperature. The detailed mechanism we suggest contains the key features of the models previously proposed in the literature by Lewis and Chalk−Harrod and adds quantitative estimates of reaction energies and barriers. On the basis of the energy profile for the catalytic cycle in the presence of inhibitor molecules and on solubility parameters for the species involved in the reaction, we conclude that the role of the inhibitors we considered is to phase-separate the catalyst from the substrate. The reaction is thus quenched by introducing a microscopic second phase that interferes with the homogeneous reaction.

1. Introduction

Hydrosilylation reactions (eq 1) are among the most important reactions in silicone and siloxane chemistry,[1] and they are extensively used as a means to form Si−C bonds. One important application of these reactions is to cross link hydrosiloxanes with vinyl terminated dimethylsiloxanes[1] for the production of protective backing surfaces in pressure sensitive adhesive labels. This often involves catalysis by late transition metals, most notably Pt, Pd, Ni, Rh, and Co[2]

$$R_3Si{-}H + H_2C{=}CHR' \rightarrow R_3Si{-}CH_2{-}CH_2R' \qquad (1)$$

Typical catalysts used for the cross linking are low valent Pt compounds. Of these, one of the best characterized is Karstedt's catalyst 2[3,4]

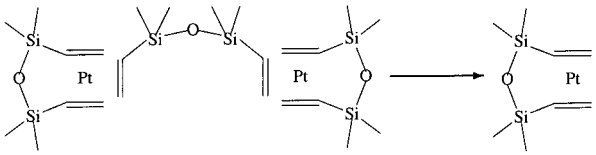

(2)

Catalyst 2 is bottled as $Pt_2[(H_2C{=}CH)(CH_3)_2SiOSi(CH_3)_2(CH{=}CH_2)]_3$. Upon solvation, the bridging ligand is released, yielding the more active form $Pt[(H_2C{=}CH)(CH_3)_2SiOSi(CH_3)_2(CH{=}CH_2)]$.

The catalyzed hydrosilylation reaction is typically fast at ambient conditions and, in the case of cross linking polymerization, results in solidification of the substrate. It is hence common practice to quench the reaction by adding inhibitors to allow easy handling and storage of the bath as a liquid. Once the bath is applied to the backing surface support, it is cured by removing the inhibitor, which activates the cross linking reaction. Typical curing conditions are 5−20 s at 100−150 °C.

In 1964, Chalk and Harrod[5,6,7] proposed a mechanism for platinum catalyzed hydrosilylation reactions based on simple elementary steps commonly observed in organometallic chemistry, such as oxidative addition and reductive elimination. A variation of the Chalk−Harrod mechanism was also proposed to explain the formation of vinylsilanes.[2,7] This version assumes an olefin attack on the Pt−Si bond that has never been observed experimentally. Although both the original and the modified Chalk−Harrod mechanisms correctly describe the hydrosilylation reaction, they fail to account for a number of phenomena observed mainly at the beginning (induction period) and the end (change in color) of the reaction.

To explain the induction period, color change, and several other effects, Lewis proposed in 1986[8,9] a radically different mechanism. He suggested that the catalytic species are colloidal platinum particles rather than organometallic complexes. He regarded the reaction as a surface, or edge, catalyzed heterogeneous process. His original mechanism became known as the Lewis mechanism. Later, he realized that although most experiments result in the formation of colloidal particles, hydrosilylation does not depend on their existence and must thus be regarded as a homogeneous process.[10] When the original Lewis mechanism is translated from the platinum surface to an organometallic compound, it becomes similar to the older Chalk−Harrod mechanism, the main difference being the order in which different ligands are coordinated and activated.

The structure of several compounds resulting from the reaction of inhibitor molecules with catalyst 2 are known from EXAFS or NMR analysis.[11] To date, however, no clear model has been formulated to rationalize the role of the inhibitors. In particular, the problem of why certain additives are better inhibitors than others has not been addressed in the literature.

In the next section, we report our computational results for each of the elementary steps involved in the Chalk−Harrod, Lewis, and a third, similar, mechanism. On the basis of these results, we conclude that all three mechanisms represent minor variations of the same catalytic cycle and that the activation energy is small. In the following section, we investigate possible roles of the inhibitors and come to the conclusion that inhibitors cannot block the active site by binding to it. In the fourth section, we report the results from solubility simulations of the various

* To whom correspondence should be addressed.
† Current address: Dip. di Chimica, Università di Modena, Via Campi 183, 41100 Modena, Italy.

10.1021/jp0128933 CCC: $22.00 © 2002 American Chemical Society
Published on Web 01/30/2002

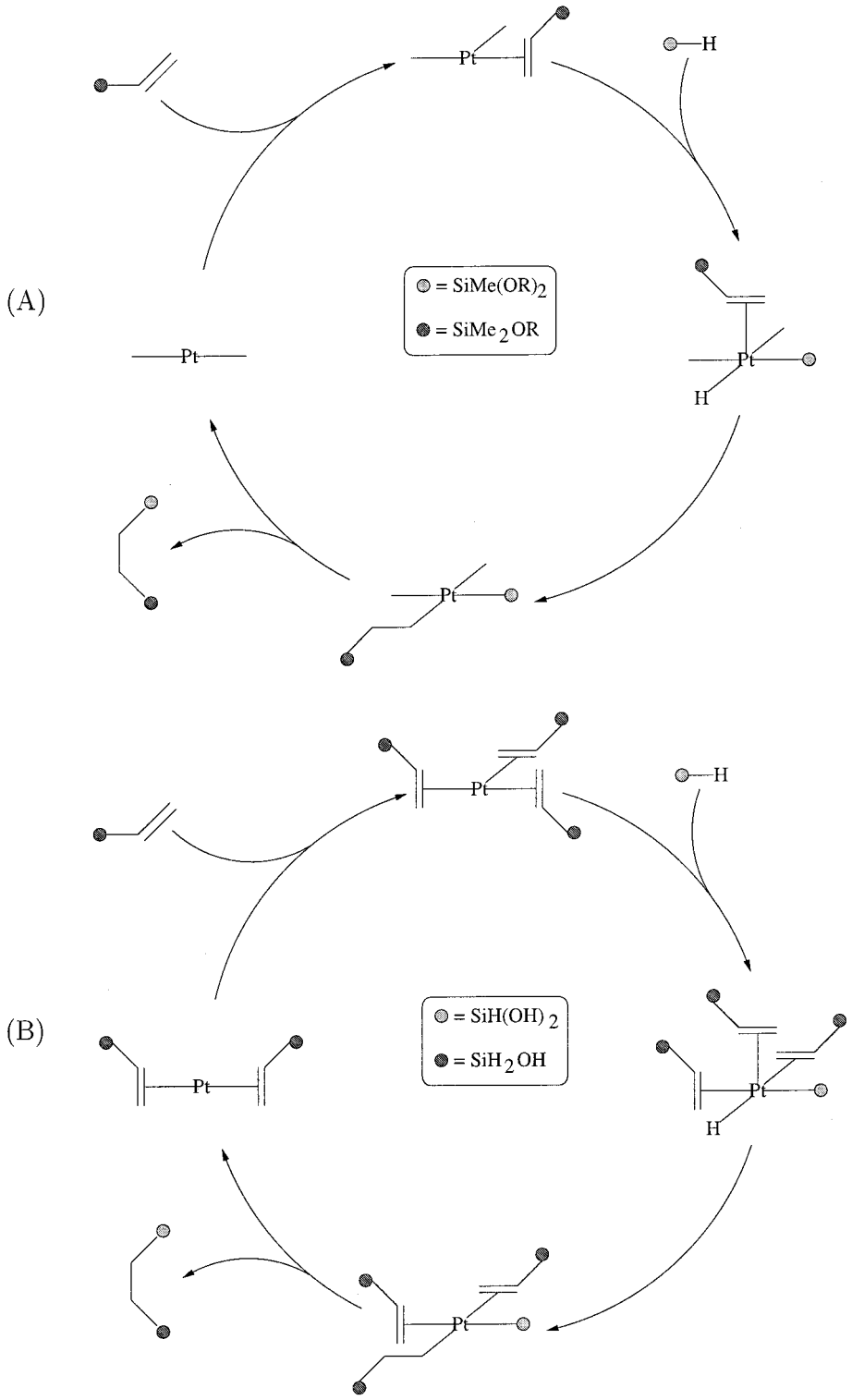

Figure 1. Chalk−Harrod mechanism as originally proposed (A) and our implementation to compute the reaction profile (B).

species involved in the reaction and conclude that inhibitors and substrate do not mix.

2. Computational Model

2.1. Computational Model. All quantum computations were obtained using the JAGUAR program suite.[12] We performed density functional theory computations using Becke's hybrid three parameter functional for the exchange[13] and Lee, Yang, and Parr functional[14] for the correlation. We used a 6-31G** double-ζ plus polarization basis set[15] on all H, C, and O atoms and a double-ζ basis set on Pt and Si.[16,17] Hay and Wadt's effective core potentials (ECP) were used to replace the inner electrons of Pt and Si.[16,17] In the case of Pt, we used the small core (core-valence) ECP, whereas for Si, we employed the large core (valence-only) ECP.

To reduce the cost of the computations, especially of geometry optimizations, we studied the effect of the catalyst only on monomers of silicon hydrides and siloxo vinyls. These were further simplified by replacing all methyl groups with hydrogens and all inactive O−SiR_3 groups with hydroxides. The

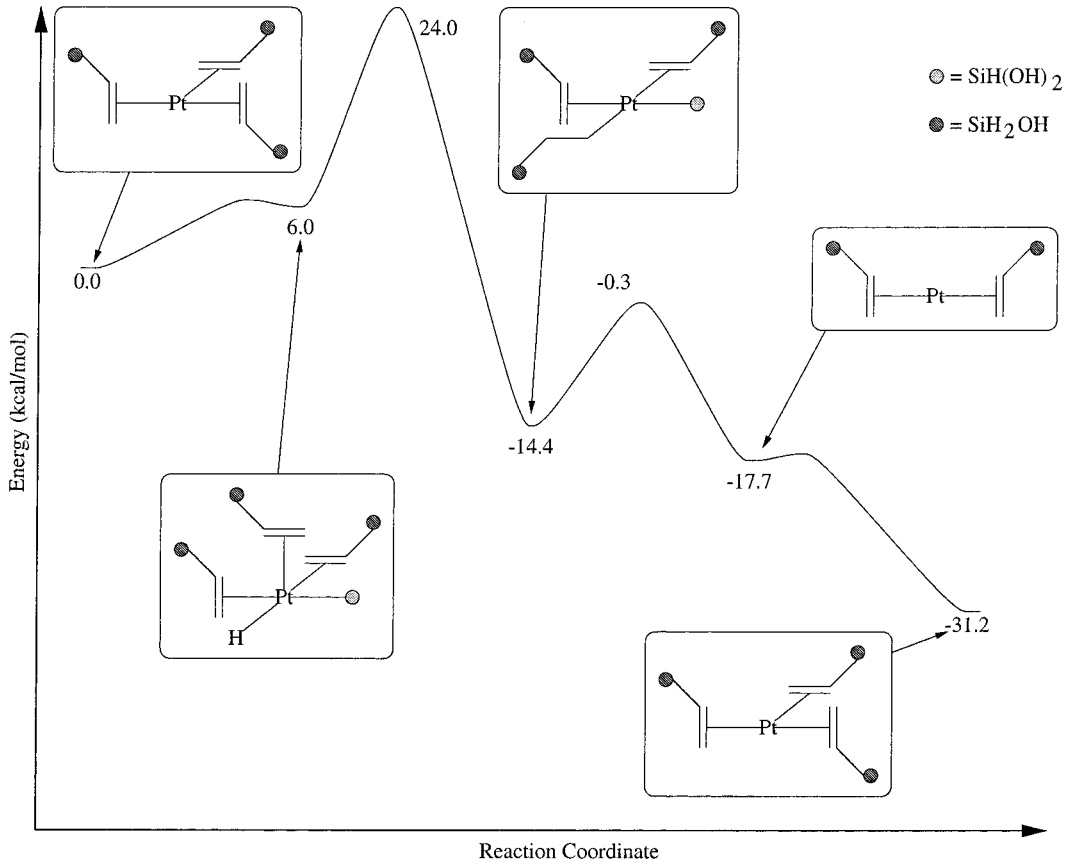

Figure 2. Energy profile for the Chalk−Harrod mechanism.

molecules used are $H_2Si(OH)_2$ and CH_2CHSiH_2OH. Being aware of the approximations made, we consistently verified that the artificial hydrogens and hydroxides so introduced would not move to sterically hindered regions or participate in hydrogen bonds.

2.2. Chalk−Harrod Mechanism. The original Chalk−Harrod mechanism[5−7] is reported schematically in Figure 1A. Starting from a Pt(0) species, it involves oxidative addition of Si−H, olefin insertion in the Pt−H bond, reductive elimination of the product, and regeneration of the catalyst. Each one of these steps has been observed in similar compounds and is generally regarded as plausible in the organometallic community. A modified version of the Chalk−Harrod mechanism has been proposed to account for the formation of vinyl-silane, which may be found in the products depending on catalyst and reactive conditions.[7] The modified version is similar to the original, except that the olefin inserts into the Pt−Si bond and the C−H bond is formed during the reductive elimination step.

To estimate the energy profile associated with the catalytic cycle, it is necessary to add explicit ligands. We thus performed computations on cycle 1B. The corresponding energy profile is reported in Figure 2. It must be noted that the pentacoordinated Pt moiety is unstable and the olefin in the axial position effectively comes off the complex. This is due to the fact that we are performing computations for gas-phase molecules whereas the real system is solvated by olefins or siloxanes. To circumvent this problem, one should modify the catalytic cycle to maintain fewer ligands around the central platinum atom. We take this approach later in this document. The energy barrier reported in Figure 2 refers to the insertion of the equatorial olefin, the insertion of the loosely bound axial olefin being higher by 1.1 kcal/mol.

The energetics for the modified Chalk−Harrod mechanism are found to be less favorable than those for the original. We could not find a stable structure for the intermediate which follows insertion in the Pt−Si bond. All calculational attempts at such an intermediate resulted in compounds where one olefin inserts in the Pt−Si bond and a second olefin inserts in the Pt−H bond, i.e., olefin insertion in the Pt−Si bond activates the Pt−H bond. The barrier for this process was found to be 31.4 kcal/mol, which is higher than the 24.0 kcal/mol obtained for insertion in the Pt−H bond alone.

According to our profile, the oxidative addition and the catalyst regeneration (olefin coordination) steps are either completely or practically barrierless. Possible rate-determining steps are the olefin insertion and reductive elimination. On the basis of this model, we thus expect most of the catalyst in solution to be found in one of the intermediates preceding these steps, i.e., with oxidation state II.

2.3. Lewis Mechanism. The original Lewis mechanism is reported in Figure 3A. Our implementation is reported in Figure 3B. It is apparent that in our implementation the Lewis mechanism differs from the Chalk−Harrod mechanism only in the order of addition of the olefin and the hydride. Since these two steps are not rate-determining, the two mechanisms are essentially the same. The energy profile, reported in Figure 4, differs from the one for Chalk−Harrod (Figure 2) only for the different starting point.

2.4. "Practical" Mechanism. To avoid pentacoordinated species, we modified the Chalk−Harrod and Lewis mechanisms by performing the insertion step before adding the fifth (olefin) ligand. This yields the catalytic cycle reported in Figure 5. We emphasize the fact that, although it is more practical to perform gas-phase computations on this cycle, once the catalyst is

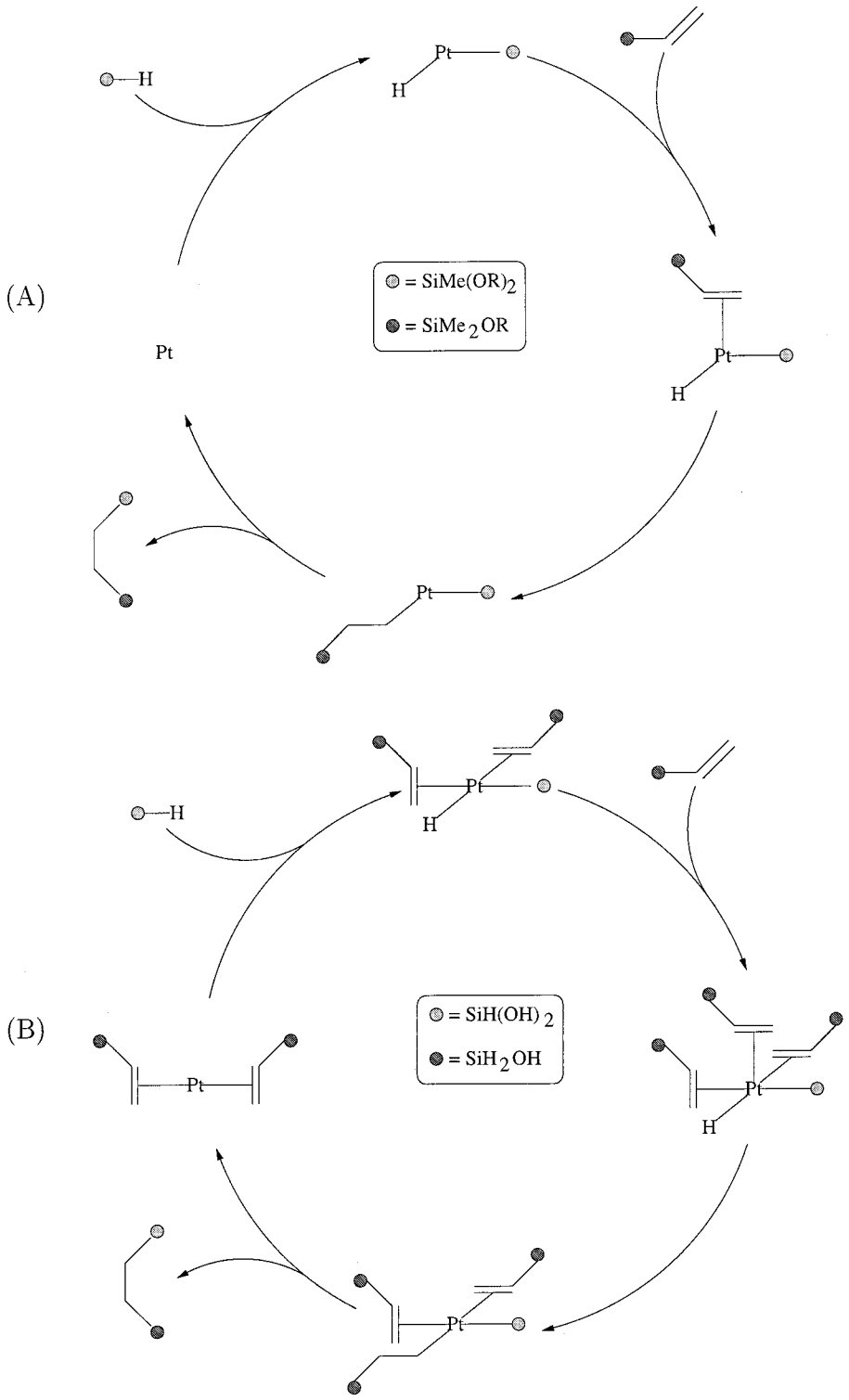

Figure 3. Lewis mechanism as originally proposed (A) and our implementation to compute the reaction profile (B).

solvated all three cycles become equivalent. In solution, there is no difference between a loosely coordinated olefin and a solvent olefin in the same position. The fact that we obtain slightly different energetics for this mechanism is a consequence of the fact that we neglect solvent effects.

The reaction profile for this mechanism is reported in Figure 6.

Since for the real system the distinction between the three mechanisms considered is immaterial, we regard them as a single catalytic mechanism. On the basis of the energy profile, we conclude that the reaction can occur via the mechanism examined with a barrier of the order of 18 kcal/mol. We expect most of the catalytically active platinum to be found in oxidation state II during the reaction. Namely, we expect it to form one of the intermediates preceding the two barriers of the cycle, labeled A and C in Figures 5 and 6. Our results indicate that the olefin insertion step is rate-determining. Hence, most of the active platinum should form intermediate A.

3. Inhibitors

3.1. Preliminary Considerations. A selection of patented inhibitors for Karstedt catalyzed hydrosilylation is reported in

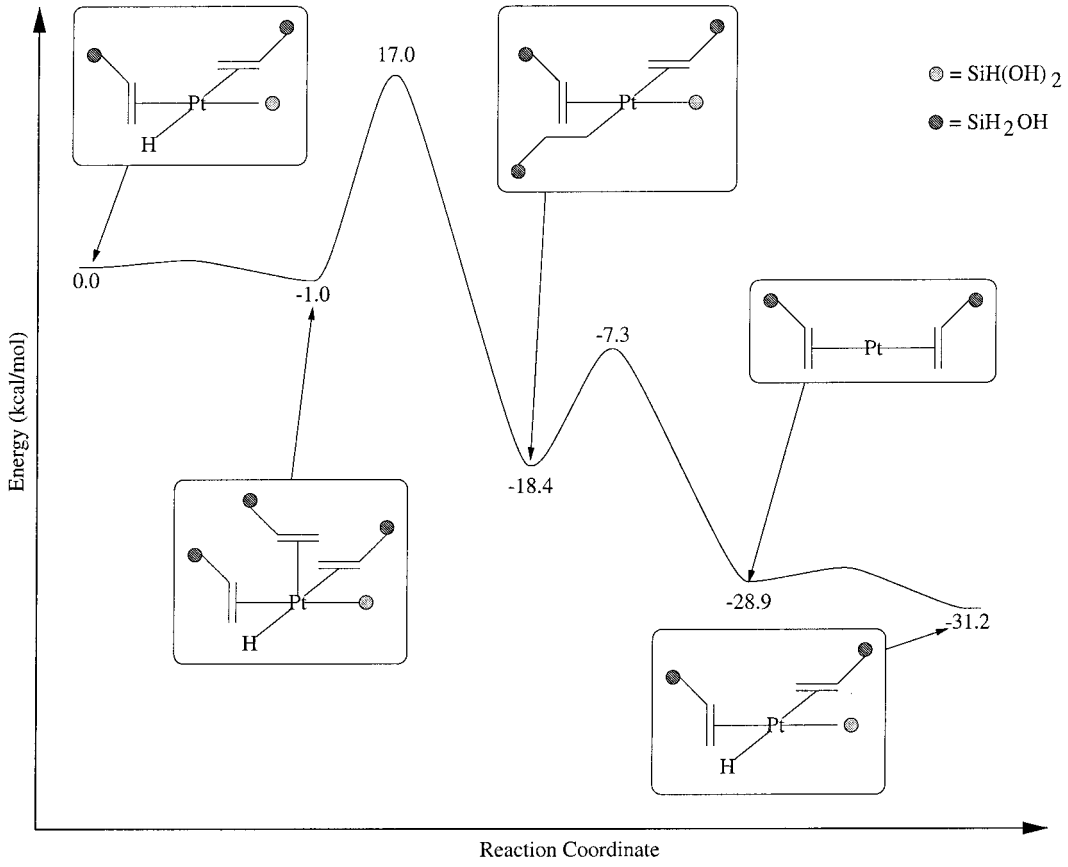

Figure 4. Energy profile for the Lewis mechanism.

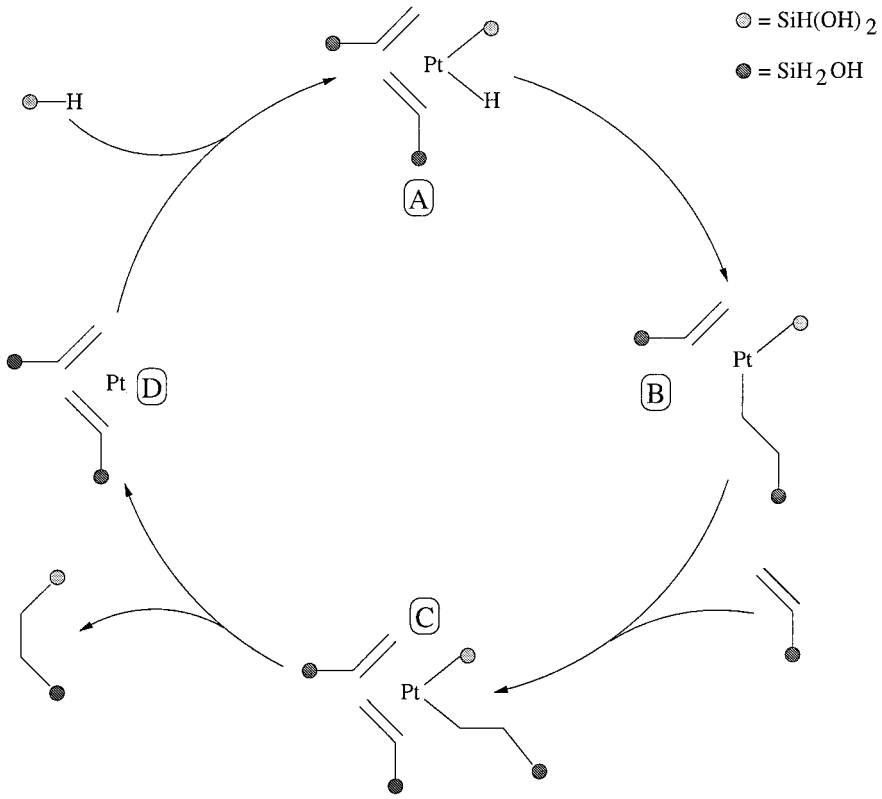

Figure 5. "Practical" mechanism used to obtain a correct description of both Chalk−Harrod and Lewis catalytic cycles. This is more practical and more accurate from a computational standpoint while representing the same chemical process.

Figure 7.[18−20] A common characteristic is the presence of C−C multiple bonds next to oxygen containing functional groups, such as alcohols and esters. The inhibitors in Figure 7 can be grouped in three main families: maleates, fumarates, and

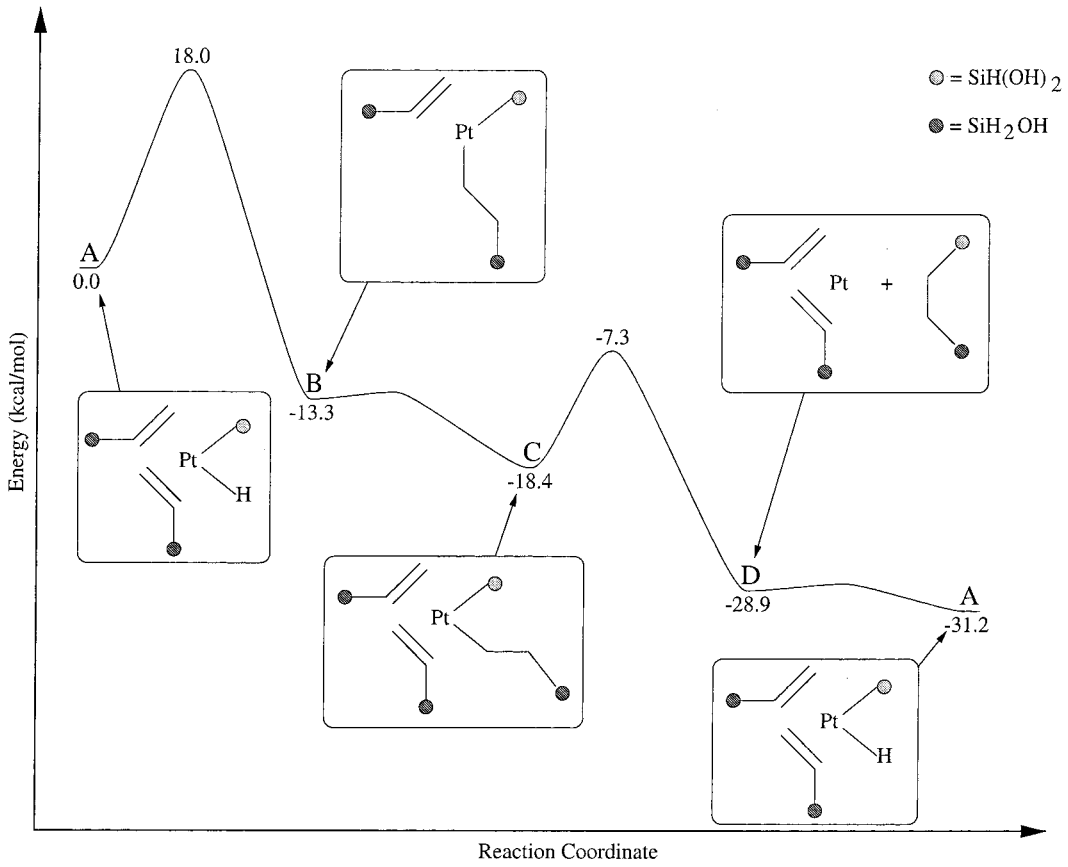

Figure 6. Energy profile for the "practical" mechanism.

β-alkynoles. Of these, maleates are typically used as single additives, whereas fumarates and β-alkynoles are sometimes used with co-inhibitors such as benzyl alcohol.

EXAFS and NMR data are available for a number of maleates and fumarates coordinating Karstedt catalyst.[11] These were obtained from binary mixtures containing only the catalyst and the inhibitor and indicate that the inhibitor's C═C bond coordinates the platinum with η^2 geometry, effectively replacing the bridging ligand in the bottled catalyst (see formula 2.) In the case of β-alkynoles, there are no structural data available due to the instability of binary mixtures of inhibitor and catalyst, which tend to polymerize and form a yellow-orange mud.

To investigate the inhibitor's behavior, we selected three simple molecules representing each of the three families reported above. Toghether with the substrate vinyl, these compounds are

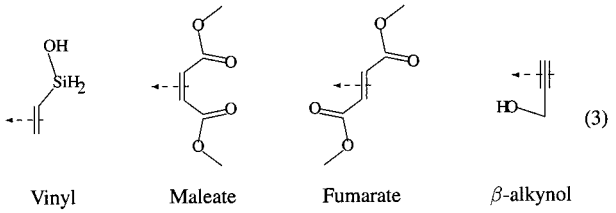

(3)

Vinyl Maleate Fumarate β-alkynol

We computed the binding energy to Karstedt catalyst of these inhibitors in a number of possible coordinating geometries. The resulting binding energies and selected equilibrium bond distances for the most stable configurations are reported in Figure 8. For maleate and fumarate, we find, in agreement with the experimental structures, that the most favorable binding configuration involves η^2 coordination of the C═C bond. A similar binding configuration is stable for β-alkynol (labeled 'unreacted' in Figure 8), although β-alkynol can, in principle, tautomerize and transfer the alcoholic hydrogen to one of the coordinating carbons. This results in a significantly more stable configuration (labeled 'reacted' in Figure 8) with platinum in oxidation state II.

With the exception of the "reacted" form of β-alkynol, all inhibitors coordinate the catalyst more weakly than the substrate vinyl. The "reacted" β-alkynol has a binding energy of 28 kcal/mol and is thus the strongest ligand in solution. We predict the formation of "reacted" β-alkynol to be irreversible, leading to poisoning of the catalyst. Due to the necessary structural rearrangement required for the reaction to occur, we expect this process to have a significant barrier. We did not investigate possible developments of the "reacted" β-alkynol, but we speculate that it may be responsible for the formation of the yellow-orange mud that is obtained from binary mixtures of Karstedt catalyst and β-alkynol.

We conclude that in the case of maleate, fumarate, and "unreacted" β-alkynol under working conditions, i.e., in the presence of vast excess of substrate vinyl with respect to the inhibitor, the inhibitor does not coordinate the catalyst. Hence, the catalyst is not inhibited by a chemical process.

4. Solubilities and Hydrophobicities

Other than affecting the ligand properties of neighboring unsaturated bonds, oxygen-containing groups alter the solubility of the molecules they are part of. We thus investigated the possibility that inhibitors (or added benzyl alcohol in the fumarate case) form a second phase around the Pt Karstedt catalyst. Evaporation of this second phase is then required to place the catalyst in contact with the reactive hydride and vinyl groups in the release coating bath. This picture is consistent

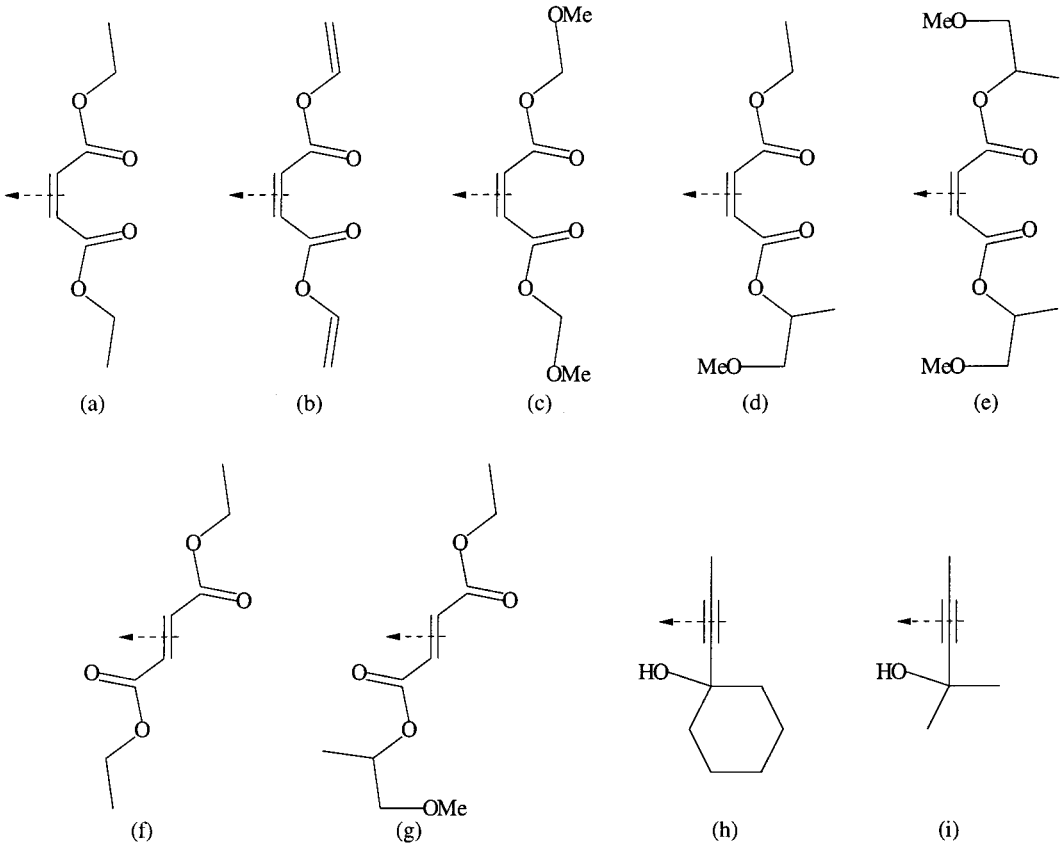

Figure 7. Selection of patented inhibitors. Arrows indicate coordinating position to the Karstedt catalyst. References are as follows: (a−e) ref 18; (f−g) ref 19; (h−i) ref 20.

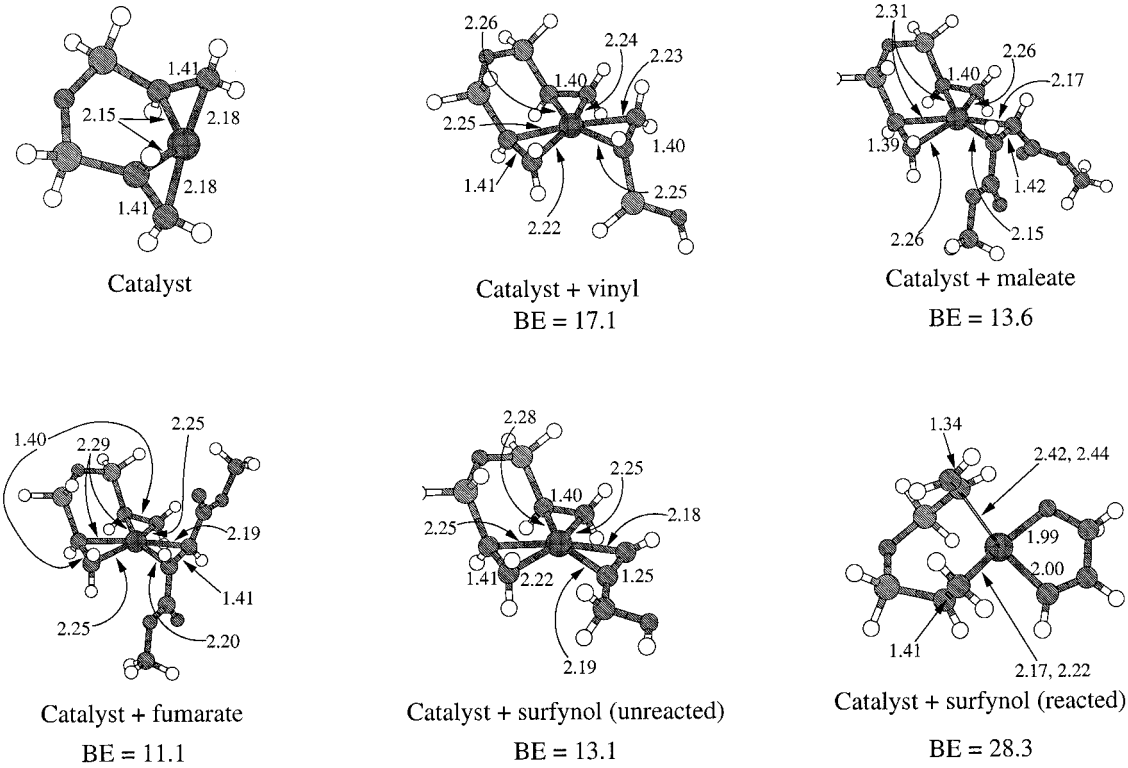

Figure 8. Binding energies (kcal/mol) and selected bond distances (Å) for Karstedt catalyst to substrate vinyl and to model inhibitor molecules.

with the extreme ratios of inhibitor to Pt (as high as 75:1) used to attain good bath life and curing rates of the catalyst formulation.

Table 1 includes estimates of the solubilities of the different components in the bath. The catalyst could not be included because platinum was not parametrized for this method and because no organometallic compounds were used to derive the parametrization for covalent species. Full geometry optimizations (B3LYP/DFT, LAV3P**) were conducted to estimate electrostatic potential atomic charges to be used in a Langevin

TABLE 1: Estimated Free Energy of Solvation and Octanol/Water Partition Coefficients Using the Langevin Dipole Model

compound	ΔG of hydration (kcal/mol)	log P octanol/water partition
	Inhibitors	
fumarate	−22.4	0.7
maleate	−23.2	0.8
β-alkynol	−17.3	0.2
benzyl alcohol	−17.6	0.7
	Bath Components	
hydride[a]	−14.7	2.2
vinyl[b]	−16.9	2.6

[a] Quantum mechanical charges (electrostatic potential fit) and solubility estimates were obtained for the trimer Me−(−SiHMe−O−)$_2$−SiHMe−Me. [b] Quantum mechanical charges (electrostatic potential fit) and solubility estimates were obtained for the trimer CH_2═CH−(−$SiMe_2$−O−)$_2$−$SiMe_2$−CH═CH_2.

dynamics[21] code trained to estimate the octanol/water partition coefficient log P according to eq 4[22]:

$$\log P = -0.205008 + 8.983102\langle 0.248 - Q^2\rangle + 0.034401\langle L + 6.472\rangle + 0.012566\langle A - 143.300\rangle - 1.213150\langle Q - 0.671\rangle + 0.373522\langle -2.311 - L\rangle - 0.023880\langle 120.151 - M\rangle \quad (4)$$

where L is the Langevin dipole energy of the charge distribution generated by the molecule, Q is the sum of nitrogen and oxygen charges, M is the molecular weight, A is the hydrophobic surface area, and $\langle\ \rangle$ indicates truncated power spline. ($\langle f(x)\rangle$ is equal to zero if the value of $f(x)$ is negative; otherwise, it is equal to $f(x)$.) This model gives a correlation coefficient $R = 0.9626$ for the published set of octanol/water partition coefficients by Bernazzani et al.[23]

The estimated log P octanol/water partition coefficients indicate that the vinyl and hydride are between 1.4 and 2.2 units of log P more hydrophobic than the inhibitors (25−150 times more soluble in octanol). Thus, these results lend credence to the proposition that the inhibitors may form a second phase in the bath formulation. Furthermore, we expect the catalyst to be preferentially solvated by the more polar inhibitor due to the presence of polarized bonds in the oxidized form of Karstedt's catalyst, most notably the Pt−H and Pt−Si bonds.

In conclusion, solubility calculations support the idea that substrate and inhibitor form a two-phase system in which the catalyst is solvated by the inhibitor. The boiling of the inhibitor phase is thus the curing rate modulator step during manufacturing. The reactants (hydride and vinyl) are 1−2 orders of magnitude more hydrophobic than any of the inhibitors considered, including benzyl alcohol.

5. Conclusions

We performed density functional computations on the main catalytic cycle for Karstedt catalyzed cross linking hydrosilylation of siloxanes. Our computations indicate, in agreement with experimental evidence, that the reaction proceeds readily at ambient conditions, with a barrier for the cycle on the order of 18 kcal/mol. We demonstrate that a set of commonly used inhibitors cannot interfere with the polymerization reaction by binding to the catalytic center.

On the basis of semiempirical solubility estimates, we conclude that the inhibitors considered are not soluble in the substrate and thus form liquid globules which physically isolate the catalyst from the substrate. Accordingly, the curing conditions are expected to depend strongly on the inhibitor's vapor pressure and boiling temperature, whereas they should depend only weakly on the inhibitor's binding energy to the catalyst.

Acknowledgment. This research is supported by grants from NPTO (DoE-FETC) and with funding from NSF (MRI and CHE 95-22179). The facilities of the MSC are also supported by grants from DoE ASCI ASAP, ARO-MURI, BP Amoco, Chevron Corp., NASA, Beckman Institute, Seiko-Epson, Exxon, Asahi Chemical, Avery-Dennison, Dow, and 3M. We thank Carl J. Bilgrien at Dow-Corning. We further thank Avery-Dennison for financial support.

References and Notes

(1) Marciniec, B. *Comprehensive Handbook on Hydrosilylation*; Pergamon Press: New York, 1992.
(2) Ojima, I. The Hydrosilylation Reaction. In *The Chemistry of Organic Silicon Compounds*; Patai, S., Rappoport, Z., Eds.; John Wiley & Sons: New York, 1989.
(3) Karstedt, B. D. U.S. Patent 3775452, 1973.
(4) Hitchcock, P. B.; Lappert, M. F.; Warhurst, J. W. *Angew. Chem., Int. Ed. Engl.* **1991**, *30*, 438.
(5) Harrod, J. F.; Chalk, A. H. *J. Am. Chem. Soc.* **1964**, *86*, 1776.
(6) Chalk, A. J.; Harrod, J. F. *J. Am. Chem. Soc.* **1965**, *87*, 16.
(7) Chalk, A. J.; Harrod, J. F. In *Organic Synthesis via Metal Carbonyls*; Wender, I., Pino, P., Eds.; John Wiley & Sons: New York, 1977; Vol 2.
(8) Lewis, L. N.; Lewis, N. *J. Am. Chem. Soc.* **1986**, *108*, 7228.
(9) Lewis, L. N. *J. Am. Chem. Soc.* **1990**, *112*, 5998.
(10) Stein, J.; Lewis, L. N.; Gao, Y.; Scott, R. A. *J. Am. Chem. Soc.* **1999**, *121*, 3693.
(11) Lewis, L. N.; Stein, J.; Colborn, R. E.; Gao, Y.; Dong, J. *J. Organomet. Chem.* **1996**, *521*, 221.
(12) *Jaguar 4.0*; Schrodinger, Inc.: Portland, Oregon, 2000.
(13) Becke, A. D. *Phys. Rev. A* **1988**, *38*, 3098.
(14) Lee, C.; Yang, W.; Parr, R. G. *Phys. Rev. B*, **1988**, *37*, 785, implemented as described in: Miehlich, B.; Savin, A.; Stoll, H.; Preuss, H. *Chem. Phys. Lett.* **1989**, *157*, 200.
(15) Here, W. J.; Pople, J. A. *J. Chem. Phys.* **1972**, *56*, 4233. Hariharan, P. C.; Pople, J. A. *Theor. Chim. Acta*, **1973**, *28*, 213. Here, W. J.; Ditchfield, R.; Pople, J. A. *J. Chem. Phys.* **1972**, *56*, 2257.
(16) Hay, P. J.; Wadt, W. R. *J. Chem. Phys.* **1985**, *82*, 299.
(17) Hay, P. J.; Wadt, W. R. *J. Chem. Phys.* **1985**, *82*, 270 and 284.
(18) Lo, P. Y. K.; Thayler, L. E.; Wright, A. P. U.S. Patent 4562096, 1985.
(19) Lo, P. Y. K. U.S. Patent 4774111, 1988.
(20) Chandra, G.; Lo, P. Y. K. U.S. Patent 4603215, 1986.
(21) Warshel, A.; Russell, S. T. *J. Am. Chem. Soc.* **1986**, *108*, 6571. Russell, S. T.; Warshel, A. *J. Mol. Biol.* **1985**, *185*, 389. Warshel, A.; Russell, S. T. *Quarterly Review of Biophysics*, **1984**, *17*, 283.
(22) Blanco, M. *Polaris Users's Guide*; Molecular Simulations Inc.: San Diego, CA, 1992; Chapter 1, p 1.18.
(23) Bernazzani, L.; Cabani, S.; Conti, G.; Mollica, V. *J. Chem. Soc., Faraday Trans.* **1995**, *91*, 649.